

# An investigation of precipitation polymerization in liquid vinyl chloride by photon correlation spectroscopy

F. M. Willmouth, D. G. Rance and K. M. Henman

Imperial Chemical Industries PLC, Petrochemicals and Plastics Division, PO Box 90, Wilton, Middlesbrough, Cleveland, TS6 8JE, UK

(Received 13 October 1983)

Simultaneous photon correlation spectroscopy and light transmittance measurements were used to follow changes in the particle size and particle number density of poly(vinyl chloride) (PVC) particles which phase separated in liquid vinyl chloride (VCM) during the early stages of bulk polymerization. The scope and limitations of these techniques for studying dynamic systems are discussed. The nature and extent of interaction forces are deduced from experimental data together with a proposed mechanism for the colloidal stability of PVC gel particles in liquid VCM.

(Keywords: vinyl chloride; poly(vinyl chloride); polymerization; photon correlation spectroscopy; colloid; coagulation)

## INTRODUCTION

The phase separation of poly(vinyl chloride) (PVC) in liquid monomer is a feature common to both the suspension and mass (bulk) polymerization processes commonly used for PVC manufacture. In the early stages of polymerization polymer appears as finely divided colloidal particles which by growth and coagulation eventually fuse to form a continuous polymer particle network. At high conversion the remaining pore space within PVC granules is to a certain extent dependent on the way in which polymer particles arrange themselves in the granule at lower conversions. The residual pore space at final conversion is an important parameter for the PVC producer in that it governs both the rate of removal of residual monomer from the final product and also the rate of ingress of plasticizer into the dried polymer powder.

In the present study, information about the formation of polymer particles during the earliest stages of vinyl chloride (VCM) polymerization has been obtained using light scattering techniques. The size and number per unit volume of precipitated gel particles were monitored as a function of time by measuring the intensity of transmitted light and simultaneously analysing scattered light using

photon correlation spectroscopy (p.c.s.) methods. The partially polymerized VCM becomes increasingly turbid as the experiment proceeds, and errors due to multiple scattering can become significant. In order to determine the range of turbidities over which reliable measurements could be made, a parallel series of experiments on model aqueous poly(butyl acrylate) lattices were carried out, in which the apparent particle size determined by p.c.s. was measured as a function of dilution. A preliminary account of this work has already been published<sup>1</sup>. Although previous and present results agree in broad outline, there are numerical discrepancies; these arise from different values for the physical properties of VCM and PVC which were used in the analysis of light scattering data. The physical properties of VCM and PVC used in the present paper are detailed in *Table 1*; they represent the most reliable data which are currently available for these materials.

Data for the rate of change of particle number with time during the early stages of polymerization provides information about the nature and extent of the interaction forces which act between monomer swollen PVC particles in liquid VCM. This information is obtained using the classical theories of colloidal stability.

Table 1 Physical properties of PVC, VCM and saturated mixtures

Property	Unit	Value at				References
		30°C	40°C	50°C	60°C	
Density of PVC ( $\rho_p$ )	kg m <sup>-3</sup>	1387	1384	1381	1378	6
Refractive index of PVC at 632.8 nm ( $m_p$ )	—	1.5383	1.5372	1.5360	1.5349	6
Density of VCM ( $\rho_m$ )	kg m <sup>-3</sup>	894	876	856	836	7, 8, 9
Refractive index of VCM at 632.8 nm ( $m_m$ )	—	1.357	1.349	1.340	1.330	10
Viscosity of VCM ( $\eta$ )	Nsm <sup>-2</sup> x 10 <sup>-4</sup>	1.80	1.69	1.60	1.53	8, 9
Density of saturated PVC/VCM Gel ( $\rho_g$ )	kg m <sup>-3</sup>	1224	1216	1208	1199	
Refractive index of saturated PVC/VCM gel at 632.8 nm ( $m_g$ )	—	1.476	1.472	1.468	1.464	

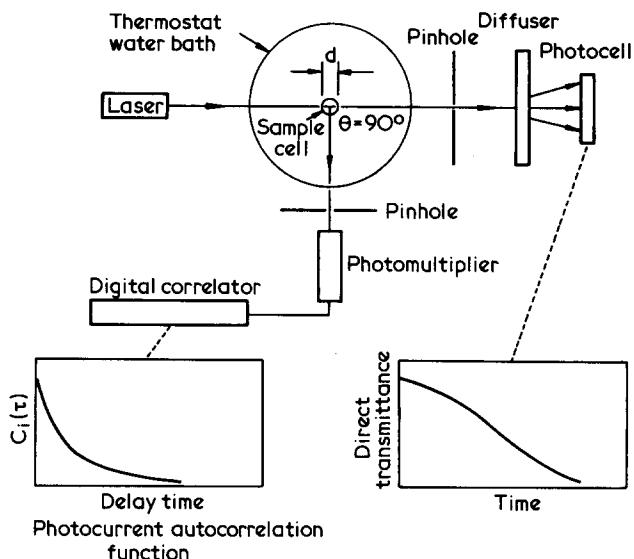


Figure 1 Schematic diagram of light scattering experiments

**THEORY**

Figure 1 shows a schematic diagram of the light scattering experiment. The polymerizing VCM is contained in a sealed cylindrical glass cell immersed in a thermostatically controlled water bath maintained at the desired polymerization temperature. The intensity of the beam directly transmitted through the cell is monitored continuously. After having been scattered through an angle  $\theta$  (maintained at  $90^\circ$  throughout), the originally monochromatic laser light has a Lorentzian frequency distribution whose half-width at half-maximum is  $DK^2$ , where  $D$  is the translational diffusion coefficient of monomer swollen nascent PVC particles within the liquid VCM, and  $K (=4\pi/\lambda \sin \theta/2)$  is the magnitude of the scattering vector,  $\lambda$  being the wavelength of the incident radiation in VCM. This scattered light is detected by a photomultiplier whose output feeds a digital correlator, and the resulting photocurrent autocorrelation function (ACF) is of the form<sup>2</sup>

$$C_i(\tau) = A + B \exp(-2DK^2\tau) \quad (1)$$

where  $A$  and  $B$  are constants, and  $\tau$  is the autocorrelation delay time.

Analysis of the ACF yields the translational diffusion coefficient, and from this the size of the gel particles may be derived using the Stokes-Einstein relation

$$D = \frac{k_B T}{6\pi\eta a} \quad (2)$$

where  $k_B$  is Boltzmann's constant,  $T$  the absolute temperature,  $\eta$  the viscosity of VCM, and  $a$  the radius of the spherical gel particle. No attempt has been made to analyse the ACF for polydispersity; we have proceeded on the simplest possible assumption that at a given instant all gel particles have identical sizes given by equation (2).

If the refractive indices of the VCM and gel are known, the particle size derived by p.c.s. may be used to calculate the particle scattering cross section ( $C_{sca}$ ) using Mie theory<sup>3,4</sup>. Thus,

$$C_{sca} = \frac{\lambda^2}{2\pi} \sum_{n=1}^{\infty} (2n+1)(|a_n|^2 + |b_n|^2) \quad (3)$$

where the scattering coefficients  $a_n$  and  $b_n$  are given by

$$a_n = \frac{\psi_n(\alpha)\psi'_n(\beta) - m\psi_n(\beta)\psi'_n(\alpha)}{\zeta_n(\alpha)\psi'_n(\beta) - m\psi_n(\beta)\zeta'_n(\alpha)} \quad (4)$$

$$b_n = \frac{m\psi_n(\alpha)\psi'_n(\beta) - \psi_n(\beta)\psi'_n(\alpha)}{m\zeta_n(\alpha)\psi'_n(\beta) - \psi_n(\beta)\zeta'_n(\alpha)} \quad (5)$$

In equations (4) and (5),  $\alpha$  and  $\beta$  are the dimensionless size parameters.

$$\alpha = k_m a = \frac{2\pi}{\lambda} a = \frac{2\pi}{\lambda_0} m_m a \quad (6)$$

$$\beta = k_g a = \frac{2\pi}{\lambda_0} m_g a \quad (7)$$

where  $m_g$  and  $m_m$  are the refractive indices of the gel particles and monomer respectively, and  $\lambda_0$  is the wavelength of the incident radiation *in vacuo*. The refractive index of the gel particle relative to the VCM is denoted by  $m (=m_g/m_m = \beta/\alpha)$ .

The Riccati-Bessel functions are derived from half integral order Bessel and Neumann functions:

$$\psi_n(Z) = \left(\frac{\pi Z}{2}\right)^{1/2} J_{n+1/2}(Z) \quad (8)$$

$$\chi_n(Z) = -\left(\frac{\pi Z}{2}\right)^{1/2} N_{n+1/2}(Z) \quad (9)$$

$$\zeta_n(Z) = \psi_n(Z) + i\chi_n(Z) \quad (10)$$

and

$$\psi'_n(Z) = \frac{d}{dZ} [\psi_n(Z)] \text{ etc.} \quad (11)$$

The attenuation of a beam traversing a suspension of scattering particles is described by<sup>3,4</sup>.

$$I = I_0 \exp(-NC_{sca}x) \quad (12)$$

where  $I_0$  and  $I$  are the incident and transmitted intensities respectively,  $N$  is the number of particles per unit volume, and  $x$  is the path length through the scattering medium (equal to the cell internal diameter  $d$  in the present experiments). Thus the number of scattering particles per unit volume can be determined from the measured direct transmittance,  $I/I_0$ , and the scattering cross-section calculated from equation (3). Finally, the volume fraction of gel particles in the polymerizing VCM ( $v_g$ ) may be calculated:

$$v_g = \frac{4\pi}{3} a^3 N \quad (13)$$

**EXPERIMENTAL**

In order to minimize multiple scattering effects, the sample tubes were chosen to be as narrow as possible consistent with ease of filling with monomer and initiator (2.5 or 3 mm internal diameter).

Di-lauroyl peroxide was used to initiate polymerization. VCM vapour was stored at stp in bulbs on a

vacuum frame. Inerts were removed from the VCM but no attempt was made to remove residual water vapour.

10  $\mu\text{l}$  samples of a 1.5% w/v solution of initiator in hexane were transferred to clean glass tubes of internal diameter 2.5 or 3 mm; solvent was evaporated by the passage of a stream of nitrogen. A sample tube containing initiator was attached to the vacuum frame and evacuated. A sample of monomer (0.15  $\text{cm}^3$ ) was transferred from the storage bulb by cooling the sample tube to  $-40^\circ\text{C}$  using a methanol-'Drikold' mixture. Using this procedure the initiator concentration was kept constant for all experiments at 0.1% w/v on monomer. The sample tube containing initiator and monomer was then frozen to liquid nitrogen temperature and sealed off by a flame so that it was short enough to be completely immersed in the water bath on the spectrometer table. Samples were allowed to warm up to  $0^\circ\text{C}$  and were stored in an ice bath until required for a polymerization run.

The specimens were illuminated by vertically plane polarized light of wavelength 632.8 nm generated by a 5 mW helium-neon laser. The directly transmitted beam was isolated from forward scattered light by a pinhole, and its intensity monitored throughout the experiment by a selenium photo-cell. Light scattered through  $90^\circ$  was detected by a photomultiplier whose output was processed by a Malvern Instruments Type K7073 48 channel digital correlator. The correlator was directly interfaced with a micro-computer which fitted the ACF to a single exponential function (equation (1)) using a generalized least squares procedure<sup>5</sup>.

Refractive indices were measured using a thermostatically controlled precision Abbe refractometer.

#### PHYSICAL DATA FOR PVC, VCM AND SATURATED MIXTURES

In order to analyse the light scattering data, certain physical properties of PVC, VCM and their equilibrium saturated mixture are required. The data used in this paper are summarized in *Table 1*. Apart from the values for the refractive index of VCM at 632.8 nm, which are previously unpublished measurements made in this laboratory, the data for pure PVC and VCM were obtained from the literature. The figures for saturated PVC/VCM gels are calculated from values for the pure components on the assumption that the volume of the gel is equal to the sum of the volumes of the two separate components. Measurements by Berens<sup>11</sup> have shown that in the range  $30^\circ\text{--}60^\circ\text{C}$ , the volume fraction of polymer in saturated VCM swollen PVC is 0.67. Thus the density of the gel is given by

$$\rho_g = 0.67\rho_p + 0.33\rho_m \quad (14)$$

and the gel refractive index by

$$\frac{m_g^2 - 1}{m_g^2 + 2} = 0.67 \left( \frac{m_p^2 - 1}{m_p^2 + 2} \right) + 0.33 \left( \frac{m_m^2 - 1}{m_m^2 + 2} \right) \quad (15)$$

#### RESULTS

##### *Investigation of multiple scattering effects using aqueous poly(butyl acrylate) lattices*

The purpose of these preliminary experiments was to determine the maximum turbidity that could be tolerated

in the polymerizing VCM before multiple scattering effects led to serious errors in the gel particle size determined by p.c.s. The most direct way of approaching this problem would have been to produce a series of samples of varying turbidity by diluting with additional pure monomer a VCM suspension in which polymerization had been terminated. However this experiment was not possible because of handling problems with VCM which has a high saturated vapour pressure at ambient temperature and because PVC particles are colloiddally unstable even when subjected to modest shear fields such as those experienced in the dilution process.

As an alternative, aqueous poly(butyl acrylate) lattices were chosen for these experiments; besides being more amenable to experimental study these lattices are at  $30^\circ\text{C}$  almost identical to monomer swollen PVC in their light scattering properties. This equivalence follows from the exact Mie scattering theory for isotropic spheres, according to which the parameters  $\alpha$  and  $\beta$  (equations (6) and (7)) determine not only the total scattering cross section (equation (3)) but also the directional distribution and state of polarization of the scattered light<sup>3,4</sup>. It follows from the definitions of  $\alpha$  and  $\beta$  that any system of isotropic spheres having a refractive index relative to the suspending liquid identical to that for monomer swollen PVC in VCM can give an identical range of values for  $\alpha$  and  $\beta$  and hence identical light scattering properties, although equivalent spheres in the two systems will not in general be of equal size.

*Table 1* shows that the refractive index of PVC gel relative to the surrounding monomer at 632.8 nm ranges from 1.088 at  $30^\circ\text{C}$  to 1.101 at  $60^\circ\text{C}$ . The refractive index of poly(butyl acrylate) and water at  $30^\circ\text{C}$  and 632.8 nm were measured as 1.4625 and 1.3309 respectively, giving a relative refractive index of 1.099, which coincides exactly with that for monomer swollen PVC in VCM at  $\approx 56^\circ\text{C}$ . The equivalent PBA sphere in water has a diameter  $\approx 0.2\%$  greater than the optically identical PVC gel sphere in VCM because of the slight difference in the absolute refractive indices between the two cases.

Two poly(butyl acrylate) lattices, each with particle sizes comparable with those of the nascent PVC gel spheres, were diluted to give two series with varying turbidities. Specimens were poured into 2.5 mm internal diameter cylinder cells and examined using an optical arrangement identical to that employed in the main polymerization experiments and illustrated in *Figure 1*. The apparent particle sizes were determined from the measured translational diffusion coefficient using a value for the viscosity of water at  $30^\circ\text{C}$  of  $7.98 \times 10^{-4} \text{ Nsm}^{-2}$ <sup>12</sup>, and are plotted in *Figure 2* against direct transmittance through the 2.5 mm thickness of latex and the equivalent turbidity derived from equation (12). For the smaller particle diameter latex, the p.c.s. size appears constant to within experimental error down to a transmittance of 0.25, falls slightly between 0.25 and 0.15, and sharply below a value of 0.10. The data for the larger particle size latex show more scatter, but the increase of  $\approx 10\%$  in apparent diameter as the direct transmittance falls from 1 to 0.15 appears to be genuine. For transmittance below 0.1, the apparent particle size again decreases rapidly.

The transmission below which serious p.c.s. particle size errors begin to arise is 0.15, and this defines the limit applied in the polymerization experiments described in the next section. For a 2.5 mm path length it corresponds

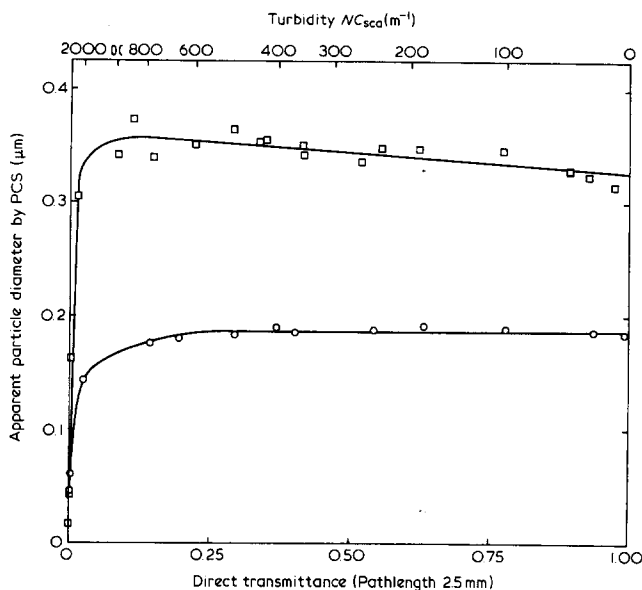


**Figure 2** Apparent particle size by p.c.s. against direct transmittance and turbidity for aqueous poly(butyl acrylate) latices; cell pathlength=2.5 mm, angle of scattering=90°

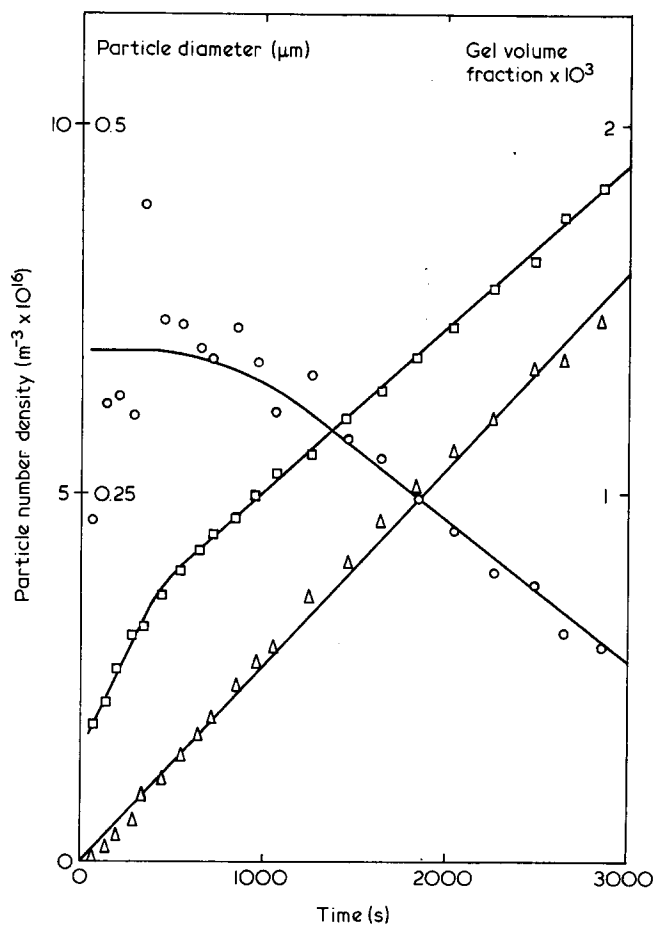


**Figure 3** Data from light scattering measurements on monomer swollen PVC particles as a function of polymerization time at 35°C: (-○-), particle number density; (-□-), particle diameter; (-△-), gel volume fraction

to a turbidity of about  $760 \text{ m}^{-1}$ . Particles of diameter  $0.184 \mu\text{m}$  have a scattering cross-section of  $4.05 \times 10^{-16} \text{ m}^2$  so that this turbidity results from a particle volume fraction of  $6.1 \times 10^{-3}$ . For the coarser latex the corresponding figures are  $4.77 \times 10^{-15} \text{ m}^2$  and

$2.6 \times 10^{-3}$ . Since the size and scattering characteristics of the PVC gel and poly(butyl acrylate) particles are closely comparable, it follows that the light scattering study of PVC polymerization is limited to gel volume fractions below a few tenths of a percent.

*Vinyl chloride polymerization in range 35°C–60°C*

The most reliable results are those obtained at lower polymerization temperatures, where the system changes least during the roughly 30 seconds required to accumulate a single ACF. Above about 60°C, polymerization proceeds so rapidly that this interval is comparable with the period during which the turbidity is low enough to permit reliable particle size measurements to be made, and higher polymerization temperatures therefore are not accessible by these techniques.

In those cases where polymerization was sufficiently slow to follow the changes in detail, a characteristic sequence of events was seen. This is illustrated in Figures 3 and 4 which show as a function of time the size, number per unit volume, and overall volume fraction of nascent PVC gel particles generated during polymerization at 35°C and 50°C, using 0.1% lauroyl peroxide as initiator. The plots of particle size consist of two distinct regions, both showing a linear increase in diameter with time and separated by a clear-cut transition. At long times, there is a rather well-defined decrease in the number of gel particles per unit volume, again approximately linear with time. At shorter time the data points are very scattered. No clear trends can be discerned, but a rough figure for

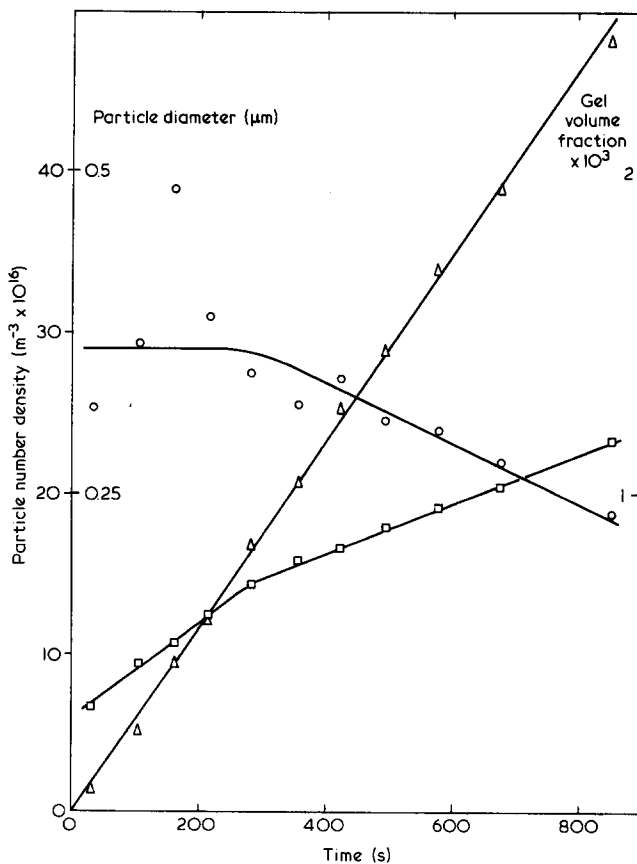


**Figure 4** Data from light scattering measurements on monomer swollen PVC particles as a function of polymerization time at 50°C: (-○-), particle number density; (-□-), particle diameter; (-△-), gel volume fraction

the initial particle number density may be determined. This scatter arises for two reasons. Firstly, at low polymer conversions the turbidity is small and consequently difficult to measure accurately. Secondly, for the small particles present early in the polymerization, the scattering cross-section varies very rapidly with sphere diameter, so that relatively small errors in particle size can lead to large errors in the particle number density deduced from equation (12). (Doubling the particle diameter from

0.05  $\mu\text{m}$  to 0.1  $\mu\text{m}$  multiplies  $C_{\text{scat}}$  by a factor of  $\approx 60$ , whereas for a corresponding increase from 0.25  $\mu\text{m}$  to 0.5  $\mu\text{m}$  the factor is only  $\approx 20$ ).

The change in the rate of increase of particle diameter occurs at the same time as the onset of the reduction in particle number per unit volume. The direct transmittances at this stage of the reaction are 0.94 and 0.78 for polymerization at 35°C and 50°C respectively, well above the level where errors due to multiple scattering effects would be expected to be significant. We believe therefore that the transition is genuine and corresponds to the agglomeration of hitherto stable growing particles.

Despite the somewhat complex changes in particle size and number density, to within the limits of experimental error, the overall gel volume fraction derived from equation (13) is a simple linear function of time in both cases. Figure 5 illustrates gel volume fraction data for a wider selection of polymerization temperatures, and shows this behaviour to be quite general. As would be expected, the rate of gel formation increases as the polymerization temperature is raised.

Table 2 summarizes results from all polymerization runs carried out using 0.1% w/v lauroyl peroxide as initiator. The agglomeration transition is defined by the point of intersection of the two linear sections of the particle size *versus* time plots rather than by the related decrease in the particle number density, whose onset is impossible to determine accurately. The origin of time is determined by extrapolating the least squares linear fit of the gel volume fraction data to zero.

The scatter in the initial particle number density figures reflects the difficulty in defining this parameter, but there appears to be a genuine increase with polymerization temperature. The gel volume fraction at the inception of agglomeration increases somewhat as the polymerization temperature is raised, but in spite of this, the marked increase in the rate of gel formation ensures that the transition time decreases. It is interesting that the particle diameter at which agglomeration commences shows no systematic variation, being  $\approx 0.2 \mu\text{m}$  throughout the temperature range studied.

The data of Figure 5 imply that at the earliest stages of polymerization, the rate of formation of PVC at a given temperature is constant. The first order rate constant for polymerization ( $k$ ) is defined by

$$\frac{dx}{dt} = kb \quad (16)$$

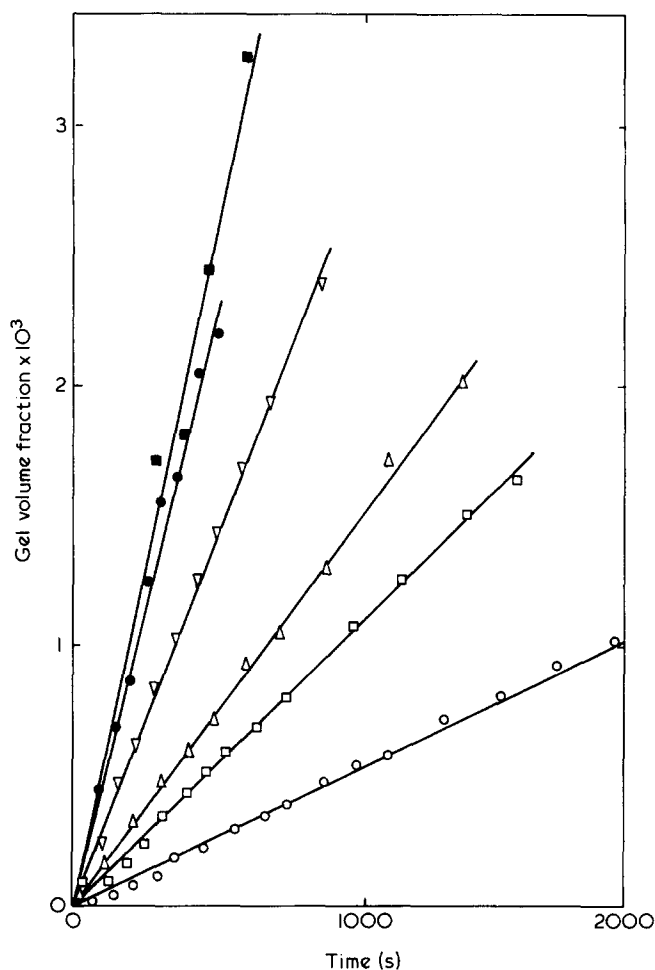


Figure 5 Volume fraction of nascent PVC gel against time for polymerization at different temperatures: (—○—), 35°C; (—□—), 40.2°C; (—△—), 45.3°C; (—▽—), 50.0°C; (—●—), 55.1°C; (—■—), 60.0°C

Table 2 Summary of results for vinyl chloride polymerization initiated by 0.1% w/v lauroyl peroxide

Polymerization temperature (°C)	Sample tube internal diameter (mm)	Rate of increase of gel volume fraction ( $\text{s}^{-1} \times 10^{-6}$ )	Initial particle number per unit volume ( $\text{m}^{-3} \times 10^{17}$ )	Agglomeration onset time (seconds)	Gel volume fraction at agglomeration onset $\times 10^4$	Particle diameter at agglomeration onset ( $\mu\text{m}$ )
35.0	2.5	0.53	0.7	450	2.4	0.19
40.0	2.5	0.76	$\approx 3$	670	5.1	0.16
40.2	2.5	1.11	1.2	380	4.2	0.19
45.3	2.5	1.53	1.0	270	4.1	0.19
45.9	2.5	1.93	3.0	300	5.8	0.16
50.0	3.0	1.89	$\approx 1$			
50.0	2.5	2.90	2.9	290	8.4	0.18
50.6	2.5	2.74	$\approx 2$	160	4.4	0.18
55.1	2.5	4.64	2.2	190	8.8	0.22
55.1	2.5	5.28	2.8	190	10.0	0.19
60.0	3.0	5.32	—			

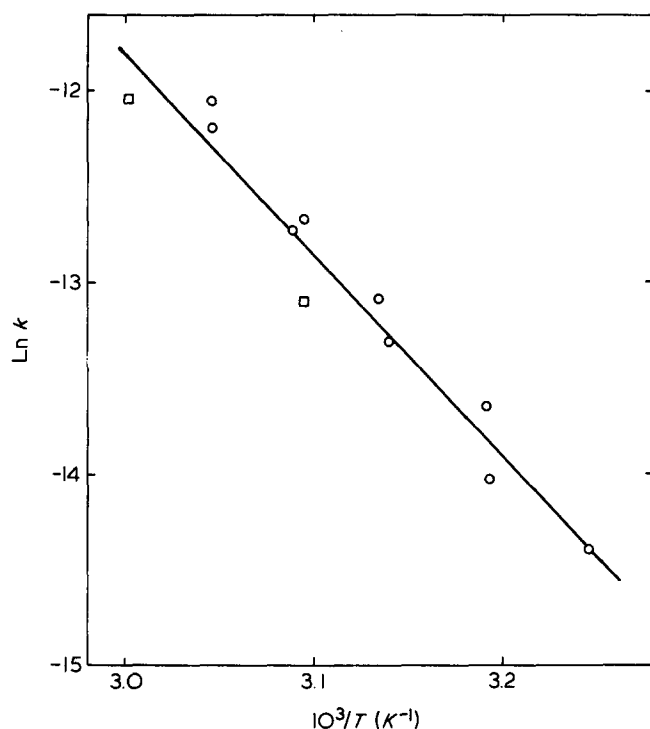


Figure 6 Arrhenius plot of  $\ln$  (polymerization rate constant) against reciprocal absolute temperature: (—○—), polymerizations in 2.5 mm i.d. tubes; (—□—), polymerizations in 3 mm i.d. tubes

where  $x$  and  $b$  are the number of moles of PVC and VCM respectively per unit volume and  $t$  is time. For the present range of very low polymer conversions,  $b$  may be regarded as a constant.

Within the range 35°C to 60°C the volume fraction of polymer in the monomer swollen gel is 0.67<sup>11</sup>, and hence the rate constant may readily be shown to be given by

$$k = 0.67 \frac{\rho_p}{\rho_m} \frac{dv_g}{dt} \quad (17)$$

where  $\rho_p$  and  $\rho_m$  are the densities of pure PVC and VCM, and  $v_g$  is the measured volume fraction of gel in the partially polymerized monomer. Figure 6 is an Arrhenius plot of  $\ln k$  versus reciprocal absolute temperature from the slope of which the activation energy for the polymerization of VCM is determined to be  $87 \pm 6 \text{ kJ mol}^{-1}$ , which is in accord with the value determined by Bengough and Norrish<sup>13</sup>. This agreement, and the simplicity and internal consistency of the results lend some credibility to our initial simplifying assumption that the precipitated gel particles are monodisperse.

## DISCUSSION

A mechanism for PVC particle formation in the monomer phase based on work reported in the literature and these experimental results appears in a previous paper<sup>1</sup>. The nucleation of polymer in bulk polymerization was studied in depth by Boissel and Fischer<sup>14</sup> who concluded from turbidity measurements that polymer precipitated from the monomer phase at conversions as low as  $10^{-3}\%$ . This is reasonable when it is realised that the length of the polymer chain at which phase separation from the monomer occurs is estimated to comprise no more than 10 monomer units<sup>1</sup>.

The first particles which appear at these low conversions are so-called basic particles (microdomains by IUPAC nomenclature), which are 10–20 nm diameter. They are believed to result from polymerization of a single radical.

The diameter of particles (0.08–0.1  $\mu\text{m}$ ) measured by p.c.s. immediately after initiation is almost an order of magnitude larger than the size of basic particles. These particles are so-called primary particle nuclei (domains by IUPAC nomenclature). Rance and Zichy<sup>1</sup> showed that the particle size and number density of primary particle nuclei, formed from basic particles, approached equilibrium within 10–20 s after initiation assuming that particles coagulate according to the second order rate equation proposed by Smoluchowski<sup>15</sup>

$$-dN/dt = k_0 N_0^2 \quad (18)$$

where  $N_0$  is the initial number of particles and  $k_0$  is the bimolecular rate constant. Hence the separate existence of basic particles is too short-lived for them to be detected by p.c.s. Therefore in these experiments p.c.s. follows the growth of primary particles and their subsequent coagulation behaviour.

Primary particles are stable to coagulation for a longer time than basic particles; Wilson and Zichy have shown<sup>16</sup> that the particles acquire a negative electrostatic charge in the early stages of polymerization. The magnitude of the negative charge on PVC particles in liquid VCM has also been investigated by microelectrophoresis experiments<sup>17</sup>. Information about the colloidal stability of particles can also be obtained from the coagulation kinetics data shown for example in Figures 3 and 4.

In the absence of any force field which results in either interparticle attraction or interparticle repulsion the rapid rate of coagulation of particles is that given in equation (18). Smoluchowski<sup>15</sup> showed that the rapid rate constant is given by

$$k_0 = 8\pi Da \quad (19)$$

where  $D$  is the translational diffusion coefficient and  $a$  the particle radius. By substituting the Stokes–Einstein equation (equation (2)) equation (19) becomes

$$k_0 = 4k_B T / 3\eta \quad (20)$$

If coagulation proceeds at a rate that is different from  $k_0$ , this provides a measure of interparticle interaction forces.

The second order rate constant  $k'_0$  for coagulation of PVC particles in VCM was calculated from the plots of particle number density against time as shown in Figures 3 and 4 using an integrated form of equation (18). The coagulation rate constant differs from that of Smoluchowski by a factor  $W$  known as the stability ratio

$$W = k_0 / k'_0 \quad (21)$$

Values of  $W$  for PVC gel particles in VCM are shown in Table 3 for VCM polymerizations over the range of temperature studied. The high positive values of  $W$  indicate the presence of a repulsive interparticle force which delays coagulation of the primary particles. Fuchs<sup>18</sup> treated slow coagulation as a diffusion problem where the collision rates of particles were considered to be

**Table 3** Estimates of the stability ratio and potential energy barrier to coagulation for nascent PVC gel particles in VCM

Polymerization temperature (°C)	Stability ratio $W$	Particle radius at onset of agglomeration ( $\mu\text{m}$ )	Average separation distance at onset of agglomeration ( $\mu\text{m}$ )	$V_t/k_B T$ ( $\Delta R = 0.1 \mu\text{m}$ )	$V_t/k_B T$ ( $\Delta R = R/2$ )
35.0	$2.1 \times 10^3$	0.10	1.27	12.0	10.2
40.0	$9.2 \times 10^3$	0.08	0.78	12.8	11.4
45.3	$9.8 \times 10^3$	0.10	1.13	13.3	11.6
50.6	$3.0 \times 10^3$	0.09	0.89	11.8	10.3
55.1	$7.0 \times 10^3$	0.10	0.80	12.3	10.9

dependent upon the potential energy of interaction  $V(R)$  between each pair and where  $R$  is the distance between the particle centres. A comparison of the coagulation rate constant from Fuchs theory with the rapid rate constant provides a further expression for the stability ratio

$$W = 2a \int_{2a}^{\infty} \exp\left(\frac{V(R)}{k_B T}\right) \frac{dR}{R^2} \quad (22)$$

It has been shown<sup>19</sup> that equation (22) can be put into a simple numerical form if the potential energy barrier is represented by a rectangular barrier of height  $V_t$  and width  $\Delta R$  at a mean distance of separation of the particle centres  $R$ . Integration of equation (22) then gives

$$W = 1 + \frac{2a\Delta R}{R^2} \left[ \exp\left(\frac{V_t}{k_B T}\right) - 1 \right] \quad (23)$$

In a medium of low dielectric constant such as VCM ( $\epsilon = 4.68$ ), the decay of potential energy with distance of interparticle separation is slow; under these conditions we might expect  $\Delta R$  to be large in comparison with the distance of interparticle separation  $H$  ( $H = R - 2a$ ). The potential energy barrier to PVC particle coagulation in monomer was estimated using equation (23) assuming either that  $\Delta R = 0.1 \mu\text{m}$  or  $\Delta R = R/2$ . Values of  $R$  were calculated from the particle number density at the onset of coagulation assuming that the particles are on average randomly distributed in the monomer and that the maximum packing fraction for randomly packed spheres is 0.6. Table 3 shows that the choice of value for  $\Delta R$  has only a small effect on the value of  $V_t/k_B T$  and that it has a numerical value of 10–14 which to a first approximation is independent of polymerization temperature.

Evidence that PVC primary particles in VCM carry a negative charge<sup>16,17,20</sup> suggests that electrostatic repulsion between the particles results in the potential energy barrier to coagulation inferred from coagulation kinetics data. It is of interest to comment on the number of elementary charges required to produce this potential energy barrier in VCM. The theory of interaction between charged colloidal particles was proposed by Derjaguin Landau Verwey and Overbeek (DLVO)<sup>21,22</sup>. According to the DLVO theory the repulsive force between two approaching particles arises from overlap of the diffuse electrical double layer surrounding the particles. For spherical particles the repulsive potential energy  $V_R$  for  $\kappa a \ll 1$  is given by

$$V_R = \frac{\epsilon a^2 \psi_0^2}{R} \beta \exp(-\kappa H) \quad (24)$$

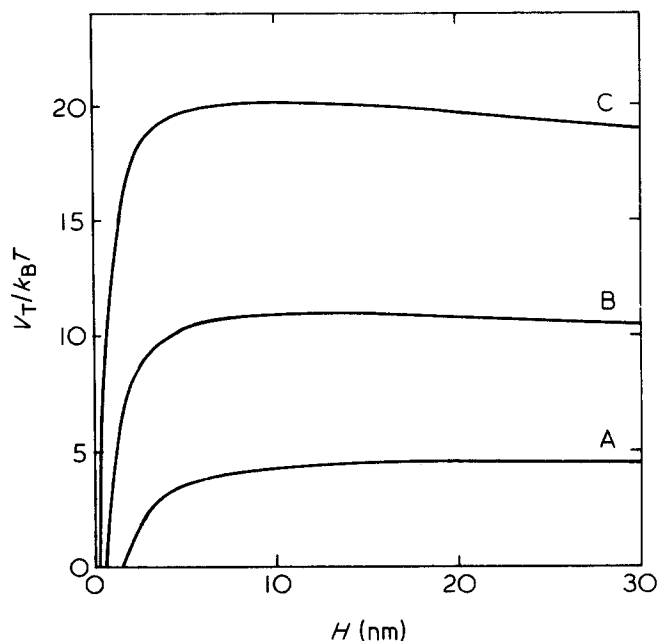


**Figure 7** Calculated total potential energy of interaction between two spheres of monomer swollen PVC in VCM against distance of interparticle separation; number of elementary charges per particle: (A), 10; (B), 15; (C), 20

where  $\psi_0$  is the surface potential of the particles, which is assumed to be low and to remain constant as they approach,  $\beta$  is a function which allows for electrical double layer distortion when they overlap and  $\kappa$  is the reciprocal double layer thickness. A similar expression to equation (24) may be written for particle–particle interaction at constant surface charge. For low dielectric constant media such as VCM, equation (24) may be simplified, assuming that  $\kappa H = 0$  and that  $\beta = 1$  i.e. that no allowance is made for double layer distortion. Under these conditions, equation (24) becomes

$$V_R = \epsilon a^2 \psi_0^2 / R = Q^2 / \epsilon R \quad (25)$$

where  $Q$  is the particle charge. Equation (25) may be readily identified as Coulombs Law for point charges.

The attractive potential energy of interaction between particles  $V_A$  which arise from van der Waals forces was described by Hamaker<sup>23</sup>; for spherical particles the simplified expression becomes

$$V_A = -Aa/12H \quad (26)$$

where  $A$  is the Hamaker constant for PVC gel particles in VCM. The Hamaker constant for this system has been calculated from optical dispersion data for PVC and VCM and allowing for the equilibrium swelling ratio of PVC by VCM ( $A = 5.0 \times 10^{-21} \text{J}$ )<sup>24</sup>.

The total potential energy of interaction  $V_t$  between two particles is given by

$$V_t = V_R + V_A \quad (27)$$

Using the approximate expressions for  $V_R$  and  $V_A$  from equations (25) and (26), plots of  $V_t/kT$  against interparticle separation are shown in *Figure 7* for particles carrying 10, 15 and 20 elementary charges per particle. The potential energy barrier to coagulation for particles carrying 15 elementary charges per particle is 11  $kT$ ; this is within the limits defined from coagulation kinetics data.

We may conclude that coagulation kinetics data for PVC particles in VCM indicate the presence of repulsive forces acting between the primary particles. This is consistent with electrostatic stabilization of the particle where they carry on average 15–17 elementary charges. The origin of charge on PVC particles in VCM is still the subject of much debate. Most authors<sup>20,24</sup> believe this is due to the adsorption of charged ions such as chloride ions which result from various dehydrochlorination reactions as polymerization proceeds. However, positive proof for particle charging mechanisms in liquid VCM will be very difficult to obtain especially where so few charges per particle are responsible for an appreciably high potential energy barrier to coagulation.

## REFERENCES

- 1 Rance, D. G. and Zichy, E. L. *Pure Appl. Chem.* 1981, **53**, 377
- 2 Chu, B. 'Laser Light Scattering', Academic Press, New York, 1974
- 3 Van de Hulst, H. C. 'Light Scattering by Small Particles', John Wiley and Sons, New York, 1957
- 4 Kerker, M. 'The Scattering of Light and Other Electromagnetic Radiation', Academic Press, New York, 1969
- 5 Crick, R. A. private communication
- 6 Ogorkiewicz, R. M. 'Engineering Properties of Thermoplastics', Wiley-Interscience, London, 1970, p 249
- 7 Dana, L. I., Burdick, J. N. and Jenkins, A. C. *J. Am. Chem. Soc.* 1927, **49**, 2801
- 8 'Ullmanns Encyklopadie der technischen Chemie', **18**, Urban and Schwarzenberg, Munich, 1967, p 87
- 9 Nehru, S. K. and Watts, A. private communication
- 10 Yearsley, F. and Zichy, E. L. private communication
- 11 Berens, A. R. *Angew. Makromol. Chem.* 1975, **47**, 97
- 12 Kaye, G. W. C. and Laby, T. H. 'Tables of Physical and Chemical Constants', Longman, London, 1973
- 13 Bengough, W. I. and Norrish, R. G. W. *Proc. Roy. Soc. London* 1950, **A200**, 301
- 14 Boissel, J. and Fischer, N. *J. Macromol. Sci.-Chem.* 1977, **A11(7)**, 1249
- 15 Smoluchowski, M. von *Z. Phys. Chem.* 1917, **92**, 129
- 16 Wilson, J. C. and Zichy, E. L. *Polymer* 1979, **20**, 264
- 17 Cooper, W. D., Speirs, R. M., Wilson, J. C. and Zichy, E. L. *Polymer* 1979, **20**, 265
- 18 Fuchs, N. *Z. Phys.* 1934, **89**, 736
- 19 Parfitt, G. D. and Peacock, J. 'Surface and Colloid Science, Vol. 10', (Ed. E. Matijevic) Plenum Press, 1978, p 163
- 20 Davidson, J. A. and Witenhafer, D. E. *J. Polym. Sci., Polym. Phys. Edn.*, 1980, **18**, 51
- 21 Derjaguin, B. V. and Landau, L. D. *Acta Physicochim URSS*, 1941, **14**, 633
- 22 Verwey, E. J. W. and Overbeek, J. Th. G. 'Theory of the Stability of Lyophobic Colloids', Elsevier, Amsterdam, 1948
- 23 Hamaker, H. C. *Physica*, 1937, **4**, 1058
- 24 Rance, D. G. and Zichy, E. L. *Polymer* 1979, **20**, 266